High-temperature expansion for Ising models on quasiperiodic tilings

1999 J. Phys. A: Math. Gen. 32 4397

(http://iopscience.iop.org/0305-4470/32/24/306)

J. Phys. A: Math. Gen. **32** (1999) 4397–4418. Printed in the UK PII: S0305-4470(99)00551-X

High-temperature expansion for Ising models on quasiperiodic tilings

Przemysław Repetowicz, Uwe Grimm and Michael Schreiber
Institut für Physik, Technische Universität, D-09107 Chemnitz, Germany

Received 4 January 1999, in final form 22 March 1999

Abstract. We consider high-temperature expansions for the free energy of zero-field Ising models on planar quasiperiodic graphs. For the Penrose and the octagonal Ammann–Beenker tiling, we compute the expansion coefficients up to 18th order. As a by-product, we obtain exact vertex-averaged numbers of self-avoiding polygons on these quasiperiodic graphs. In addition, we analyse periodic approximants by computing the partition function via the Kac–Ward determinant. It turns out that the series expansions alone do not yield reliable estimates of the critical exponents. This is due to the limitation on the order of the series caused by the number of graphs that have to be taken into account, and, more seriously, to rather strong fluctuations in the behaviour of the coefficients. Nevertheless, our results are compatible with the commonly accepted conjecture that the models under consideration belong to the same universality class as those on periodic two-dimensional lattices.

1. Introduction

Since the discovery of quasicrystals in the early 1980s [1–4] considerable attention has been paid to the magnetic properties of these materials. While many quasicrystals contain atoms (such as Fe, Mn or rare-earth elements) that carry local magnetic moments, these are usually screened very effectively and consequently one finds a weak paramagnetic or diamagnetic behaviour, see e.g. [5, 6]. Recently, however, there has been ample experimental evidence for magnetic ordering in quasicrystals, including ferrimagnetic [7], ferromagnetic [8], antiferromagnetic [9], and spin-glass behaviour [10–13], though some results are still discussed controversially, see e.g. [14, 15], in particular with regard to the importance of crystalline phases present in the samples.

Even before magnetic ordering in quasicrystals had been observed experimentally, theoretical investigations on the influence of quasiperiodic order on magnetic properties commenced. In most cases, the models considered were either one-dimensional quantum spin chains with aperiodic sequences of coupling constants or classical Ising models on two-dimensional quasiperiodic graphs; we refer the reader to the recent review [16] for a rather complete list of references. Recently, a symmetry classification scheme for magnetically ordered quasicrystals has been proposed [17].

In this context, it is one of the central questions whether quasiperiodic order influences the universal properties at the phase transition, such as the critical exponents, in comparison with the periodic case. There is a heuristic criterion due to Luck [18] on the relevance of aperiodicity, extending an old result of Harris [19] for random defects, see also [20] for a closer examination of the underlying scaling arguments. According to this criterion, the 'topological disorder' encountered in two-dimensional quasicrystals, generated by the cut-and-project method, is

0305-4470/99/244397+22$19.50

irrelevant; and hence an Ising model on a quasiperiodic tiling should belong to the same universality class as the Ising model on the square lattice. Clearly, non-universal properties do, in general, depend on the particular system under consideration. For instance, the location of critical points of lattice models depends in a systematic way on the structure of the graph on which the model is defined, see [21] and references therein.

In this paper, we consider high-temperature expansions of the free energy for zero-field Ising models on two planar quasiperiodic graphs, the decagonal Penrose [22, 23] and the octagonal Ammann–Beenker [24–26] tiling. The technique of high-temperature expansions is well known, see e.g. [27]; it was developed several decades ago and has since been applied to a variety of periodic lattices in both two and three dimensions. With regard to previous work on high-temperature expansions of quasiperiodic Ising models, we are only aware of two articles by Abe and Dotera [28,29] who compute the expansion of the free energy up to the eighth order for the Penrose tiling and its dual, and of a few numerically calculated expansion coefficients for the susceptibility for the Penrose case [30]. Employing a systematic procedure, we are able to compute the exact values of the coefficients up to the 18th order for both the Penrose and the Ammann–Beenker tiling. This requires much more effort than the calculation for periodic lattices, because the number of graphs that one has to take into account grows tremendously with the order. Although our expansions are still not yet sufficient to extract good estimates for the critical temperatures or the critical exponents, we can show that our results are consistent with those obtained by different methods.

From the high-temperature expansion of the free energy, one can compute the correlation critical exponent ν. In order to check universality, one would have to consider two independent critical exponents. In principle, we could compute a magnetic exponent by using the high-temperature series for the magnetic susceptibility by similar means. However, more general graphs have to be considered in that case, and the number of graphs that one has to take into account is again much larger than the number of those that contribute to the series expansion of the free energy. This means that, with a comparable effort, it would not be possible to obtain the susceptibility series even to 18th order. Therefore, and in view of the rather limited predictive power that our 18th order high-temperature series for the free energy proves, we restrict ourselves to the simpler case and exclusively treat the series expansion for the free energy.

Presently, the most accurate data on the transition temperature and the critical exponents stem from Monte Carlo simulations [31–34]. Besides graphical expansions and Monte Carlo simulations, further methods have been employed to gain information about the critical behaviour of quasiperiodic Ising models. First of all, exactly solvable cases can be constructed as, for instance, the Ising model on the so-called labyrinth tiling [35], see also [16, 36] for further examples. These models correspond to particular choices of coupling constants, restricted by the requirement of integrability, and thus might not be representative for the general situation. For the solvable models based on the idea of 'Z-invariance', see [16] and references therein, the critical behaviour necessarily is the same as for the periodic case, but one does not get a clue whether this extends to the general case, or whether it is at least the generic situation. Second, there is an interesting approach using Lee–Yang zeros [37], which are complex roots of the partition function in certain variables. Simon and Baake [38, 39] calculated the zeros of the partition function for a large patch of the Ammann–Beenker tiling numerically and drew conclusions about the critical temperature and the critical exponents. Furthermore, renormalization group techniques were applied to study the Ising model on two-dimensional quasiperiodic tilings [40]. In that case, one exploits the self-similarity of quasiperiodic tilings, which translates into a renormalization procedure that, however, can only be treated approximately in general. We note that for one-dimensional quantum Ising

chains with aperiodically modulated coupling constants, corresponding to two-dimensional layered Ising models, renormalization techniques may yield exact results for the critical behaviour [41, 42]. In this case, the modulation is one-dimensional, and in accordance with Luck's criterion [18] one finds that the critical behaviour depends on the fluctuations of the aperiodic sequence of coupling constants.

So far, all results appear to be in accordance with Luck's criterion, including a recent Monte Carlo study of the three-state Potts model on the Ammann–Beenker tiling [43]. Still, most approaches are based on numerical or approximative treatments. It is our aim to obtain the exact values of the coefficients for the high-temperature expansions. However, we should note that it is, of course, not possible to reconstruct the singular part of the free energy from a finite-degree polynomial comprising the first terms of a high-temperature series, and that conclusions on the critical behaviour of the model drawn from this approach involve extrapolations and cannot therefore be exact.

The paper is organized as follows. In the subsequent section, we briefly recall the graphical high-temperature expansion of Ising models. In section 3, we discuss the generation of subgraphs of quasiperiodic tilings and the computation of their occurrence frequencies. Then, in section 4, we present our results for the coefficients of the high-temperature expansions for the Penrose and the Ammann–Beenker tiling. The corresponding implications for the critical behaviour are discussed in section 5. In section 6, we compare our results with exact calculations of the partition functions of periodic approximants. Finally, in section 7, we present our conclusions.

2. High-temperature expansion

We now give a brief account of the high-temperature expansion for the free energy of an Ising model on a graph without an external field [27]. Let us consider a finite graph $\mathcal{G}$ containing N sites (vertices) with M pairs of neighbouring vertices connected by bonds. We emphasize that, throughout this paper, the notion of neighbouring vertices refers to vertices connected by a bond, and not to the geometric distance between the vertices. For instance, in the Penrose tiling discussed below, the short diagonal of the small rhombus corresponds to the smallest distance between vertices, but does not constitute a bond. At a vertex j, we place an Ising spin $\sigma_j \in \{\pm 1\}$; and two spins σ_j and σ_k located at neighbouring vertices j and k interact with a coupling constant J which we assume to be independent of the position. Hence the energy of a spin configuration $\boldsymbol{\sigma} = \{\sigma_1, \sigma_2, \ldots, \sigma_N\}$ on $\mathcal{G}$ is given by

$$E(\boldsymbol{\sigma}) = -J \sum_{\langle j,k \rangle} \sigma_j \sigma_k \tag{2.1}$$

where we sum over all pairs $\langle j, k \rangle$ of neighbouring vertices connected by bonds as mentioned above. The logarithm of the partition function

$$\begin{aligned} Z(\mathcal{G}) &= \sum_{\boldsymbol{\sigma}} \exp[-\beta E(\boldsymbol{\sigma})] \\ &= [\cosh(\beta J)]^M \sum_{\boldsymbol{\sigma}} \prod_{\langle j,k \rangle} [1 + \sigma_j \sigma_k \tanh(\beta J)] \end{aligned} \tag{2.2}$$

is, apart from a factor $-1/\beta$, the free energy. It can be expanded as

$$\ln Z(\mathcal{G}) = N \ln 2 + M \ln[\cosh(\beta J)] + N \sum_{n=1}^{\infty} g_n w^n \tag{2.3}$$

where $\beta = 1/k_B T$ with Boltzmann's constant k_B and temperature T. The expansion variable

$$w = \tanh(\beta J) \tag{2.4}$$

is small for high temperature, hence the notion high-temperature expansion. The expansion coefficients g_n are related to the number of subgraphs of $\mathcal{G}$ containing n bonds.

The terms in the expansion (2.3) can be rearranged in a different fashion which is more convenient for our needs (see p 382 in [27])

$$\begin{aligned}\ln \tilde{Z}(\mathcal{G}) &= \ln Z(\mathcal{G}) - N \ln 2 - M \ln [\cosh (\beta J)] \\ &= N \sum_{n=1}^{\infty} g_n w^n = \sum_r (c_r; \mathcal{G}) k_r(w)\end{aligned} \tag{2.5}$$

where we now sum over all *connected* subgraphs c_r of $\mathcal{G}$. The quantity $(c_r; \mathcal{G})$ denotes the so-called *lattice constant* of c_r in $\mathcal{G}$, counting the number of ways c_r can be embedded in $\mathcal{G}$. The weight functions $k_r(w)$ depend only on c_r, not on $\mathcal{G}$. In our case, without external field, we can restrict the sum to so-called *star graphs*. These are graphs that cannot be dissected into two disjoint subgraphs by eliminating a single vertex.

The weight functions $k_r(w)$ in equation (2.5) can be calculated from the partition function $\tilde{Z}(c_r)$ of the subgraph c_r. For this aim, let us generate all star subgraphs and arrange them in a sequence $\{c_r\}_{r=1,2,\ldots}$ such that c_s cannot be embedded in c_r for $r < s$. In other words, the lattice constant $(c_s; c_r)$ may be non-zero only if $s \leqslant r$, which, in general, does not determine the sequence uniquely. Having arranged the subgraphs in such a way, the expansion (2.5) for a subgraph c_r gives

$$\ln \tilde{Z}(c_r) = \sum_{s=1}^{r} (c_s; c_r) k_s(w) \tag{2.6}$$

and, taking into account that $(c_r; c_r) = 1$, we obtain the corresponding weight $k_r(w)$

$$k_r(w) = \ln \tilde{Z}(c_r) - \sum_{s=1}^{r-1} (c_s; c_r) k_s(w) \tag{2.7}$$

expressed in terms of lattice constants $(c_s; c_r)$ and weights $k_s(w)$ with $s < r$. Therefore, we can successively compute the weights $k_r(w)$ provided we know the partition function $\tilde{Z}(c_r)$ and the lattice constants $(c_s; c_r)$ of all star graphs c_s that are subgraphs of c_r.

We note that we can rearrange the sum in equation (2.5) as

$$\ln \tilde{Z}(\mathcal{G}) = \sum_{n=3}^{\infty} \sum_r \sum_s (c_{r,s}^{(n)}; \mathcal{G}) k_{r,s}^{(n)}(w) \tag{2.8}$$

where r labels closed loops $l_r^{(n)}$ consisting of n bonds, and $c_{r,s}^{(n)}$ are all possible complete 'fillings' of the loop $l_r^{(n)}$. By 'fillings' of a loop we mean all proper subgraphs of $\mathcal{G}$ which have the loop as their boundary. Here, the functions $k_{r,s}^{(n)}(w)$ have the form

$$k_{r,s}^{(n)}(w) = w^n + \mathrm{O}(w^{n+1}). \tag{2.9}$$

Hence, truncating the sum over n in equation (2.8) yields all terms in the expansion up to nth order in w. The calculation of the weight functions $k_{r,s}^{(n)}(w)$ can be performed in analogy to that of the weight functions $k_r(w)$ (2.7).

In summary, in order to calculate the high-temperature expansion (2.8) of the Ising model to order $n_{\max}$ we have to perform the following steps:

(i) generate all loops $l_r^{(n)}$ in the graph $\mathcal{G}$ consisting of $n \leqslant n_{\max}$ bonds;
(ii) construct all fillings $c_{r,s}^{(n)}$ of $l_r^{(n)}$;
(iii) calculate $\ln \tilde{Z}(c_{r,s}^{(n)})$, the logarithm of the partition function for the subgraphs $c_{r,s}^{(n)}$;
(iv) calculate the lattice constants $(c_{r,s}^{(n)}; \mathcal{G})$ and $(c_{r',s'}^{(n')}; c_{r,s}^{(n)})$;

(v) compute the weight functions $k_{r,s}^{(n)}(w)$ by successive use of the analogue of (2.7);
(vi) calculate the expansion (2.8).

We are now in the position to apply this scheme to the case of quasiperiodic graphs.

3. Frequencies of subgraphs of quasiperiodic tilings

In fact, we want to obtain the expansion (2.5) for the Ising model on an infinite quasiperiodic graph $\mathcal{G}$. Therefore, we have to compute the corresponding 'averaged lattice constants' per vertex

$$\langle c_r; \mathcal{G}\rangle := \lim_{N\to\infty} \frac{1}{N}(c_r; \mathcal{G}_N) \tag{3.1}$$

where $\mathcal{G}_N$ denotes finite patches with N vertices approaching the infinite graph $\mathcal{G}$. In other words, we need to calculate the occurrence frequency of a subgraph c_r in the infinite graph $\mathcal{G}$. The main challenge now is to compute these quantities for a given quasiperiodic graph and all of its subgraphs up to a certain size.

For quasiperiodic graphs generated by the cut-and-project method [44] the frequencies of subgraphs can be computed exactly. In the cut-and-project method, one starts from a higher-dimensional periodic lattice, and projects a certain part of it onto a lower-dimensional 'physical' or 'parallel' space $E_\parallel$. For the two cases of interest, the Penrose and the octagonal Ammann–Beenker tiling, the lattices have to be at least four-dimensional, the minimal choice being the root lattice A_4 for the Penrose case [45] and the hypercubic lattice $\mathbb{Z}^4$ for the octagonal case [25]. The root lattice A_4 can be considered as a sublattice of $\mathbb{Z}^5$, wherefore the latter, albeit not minimal, is frequently used to generate the Penrose tiling. The physical space $E_\parallel$ is determined as an invariant subspace with respect to the relevant subgroup (in our examples the dihedral groups D_5 and D_8, respectively) of the point group of the periodic lattice. Its orthogonal complement, the perpendicular space $E_\perp$, is then also an invariant subspace of this symmetry. The quasiperiodic tiling is now obtained by projecting all those lattice points onto $E_\parallel$ whose projection onto $E_\perp$ falls into a certain set called the 'window' or 'acceptance domain' A. In the minimal case, this acceptance domain has the same dimension as $E_\perp$; however, if we project the Penrose tiling from the hypercubic lattice $\mathbb{Z}^5$, the perpendicular space is three-dimensional and the acceptance domain consists of four regular pentagons P_m ($m = 1, 2, 3, 4$) situated on equidistant, parallel planes, and two isolated points (P_0 and P_5), see figure 1. For the Ammann–Beenker tiling, the situation is simpler; the acceptance domain, which is obtained as the projection of the four-dimensional hypercube to $E_\perp$, is a regular octagon O.

Now, considering an arbitrary motive c consisting of a collection of p points $c = \{\boldsymbol{r}_\parallel^{(i)}; 1 \leqslant i \leqslant p\}$ in physical space, we can compute its occurrence frequency, i.e., how often translated copies of the point set occur in the infinite tiling. Associated to the set c of points in physical space is a corresponding acceptance domain $A(c) \subset A$ in perpendicular space, obtained by intersecting p copies of the acceptance domain A shifted appropriately with respect to each other. This corresponds to the acceptance domain filled by choosing a reference point of the motive c, and, for all occurrences of the motive in an infinite tiling, lifting the positions of this reference point to the higher-dimensional lattice and projecting to $E_\perp$. Hence, the area of $A(c)$, divided by the area of A, is the occurrence frequency of our motive, as follows from the uniform distribution on the acceptance domain, see [46] and references therein.

In the Penrose case, the acceptance domain $A(c)$ consists of four pieces $A_m(c) \subset P_m$ ($m = 1, 2, 3, 4$) which have to be taken into account. They are given by

$$A_m(\{\boldsymbol{r}_\parallel^{(i)}\}) = \bigcap_i \{P_{m+t^{(i)}} - \boldsymbol{r}_\perp^{(i)}\} \tag{3.2}$$

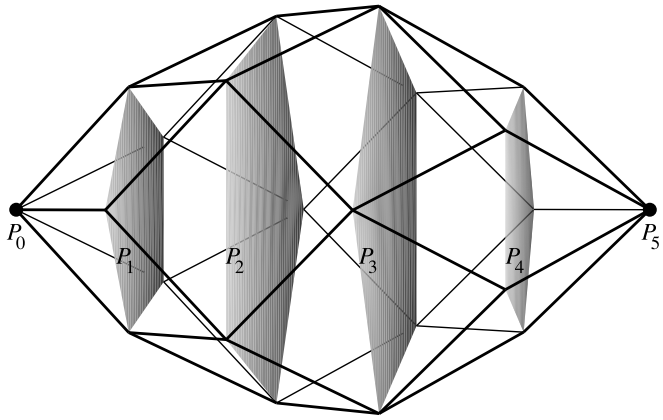

Figure 1. The acceptance domain of the Penrose tiling, consisting of four regular pentagons P_1, P_2, P_3, P_4, and two isolated points P_0, P_5, situated on equidistant parallel planes in the three-dimensional space $E_\perp$. The polytope spanned by the lines is the projection of the five-dimensional hypercube to $E_\perp$.

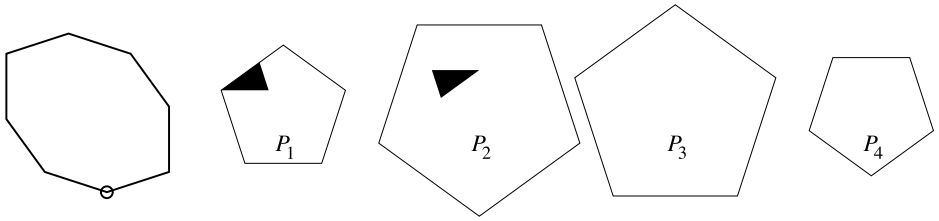

Figure 2. The 'fattest' loop of length eight in the Penrose lattice and its acceptance domain (black polygons) with respect to the reference point marked by the circle (○). The area fraction is $\tau - \frac{8}{5} \simeq 0.0180$ where $\tau = (1+\sqrt{5})/2$ is the golden ratio. The symmetry factors read $R = 5$ and $S = 1$, thus the occurrence frequency of this loop in the Penrose tiling, in an arbitrary orientation, is $5\tau - 8 \simeq 0.0902$.

where $P_m = \emptyset$ if $m \notin \{0, 1, 2, 3, 4, 5\}$. The coordinates $\boldsymbol{r}_\parallel^{(i)} \in E_\parallel$ and $\boldsymbol{r}_\perp^{(i)} \in E_\perp$ have the form

$$\boldsymbol{r}_\parallel^{(i)} = \sum_{j=0}^{4} n_j^{(i)} \begin{pmatrix} \cos\frac{2\pi j}{5} \\ \sin\frac{2\pi j}{5} \end{pmatrix} \qquad \boldsymbol{r}_\perp^{(i)} = \sum_{j=0}^{4} n_j^{(i)} \begin{pmatrix} 1 \\ \cos\frac{4\pi j}{5} \\ \sin\frac{4\pi j}{5} \end{pmatrix} \tag{3.3}$$

with integer coefficients $n_j^{(i)}$ which correspond to the coordinates of the lattice point in $\mathbb{Z}^5$ that projects to $\boldsymbol{r}_\parallel^{(i)}$. The first component of $\boldsymbol{r}_\perp^{(i)}$,

$$t^{(i)} = \sum_{j=0}^{4} n_j^{(i)} \tag{3.4}$$

denotes the so-called translation class of the point $\boldsymbol{r}_\parallel^{(i)}$, which just labels the part of the acceptance domain $P_{t^{(i)}}$ where the corresponding perpendicular projection lies. In figures 2 and 3, we show two examples where the motives are the 'fattest' loops, in terms of the enclosed area, of length 8 and 10 in the Penrose tiling that contribute to the high-temperature expansion.

For the eightfold Ammann–Beenker case there is only one acceptance domain O, hence

$$A(\{\boldsymbol{r}_\parallel^{(i)}\}) = \bigcap_i \{O - \boldsymbol{r}_\perp^{(i)}\} \tag{3.5}$$

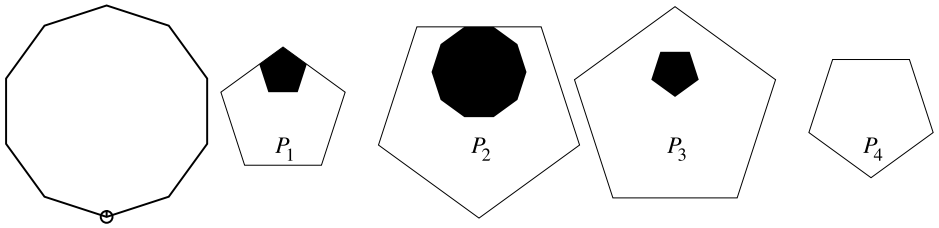

Figure 3. As figure 2, now for the 'fattest' loop of length ten. Here, the area fraction is $(14\tau - 22)/5 \simeq 0.1305$, and the symmetry factors read $R = S = 1$.

where the projections to $E_\parallel$ and $E_\perp$ are given by

$$\boldsymbol{r}_\parallel^{(i)} = \sum_{j=0}^{3} n_j^{(i)} \begin{pmatrix} \cos\frac{\pi j}{4} \\ \sin\frac{\pi j}{4} \end{pmatrix} \qquad \boldsymbol{r}_\perp^{(i)} = \sum_{j=0}^{3} n_j^{(i)} \begin{pmatrix} \cos\frac{3\pi j}{4} \\ \sin\frac{3\pi j}{4} \end{pmatrix}. \tag{3.6}$$

Here, $n_j^{(i)} \in \mathbb{Z}$ denote the coordinates of the lattice point in $\mathbb{Z}^4$ that projects to $\boldsymbol{r}_\parallel^{(i)}$.

The acceptance domains of a motive c are intersections of convex polygons and hence themselves polygonal, see figures 2 and 3. It is readily seen that the coordinates of the vertices of the acceptance domains belong to certain extensions of the field of rational numbers $\mathbb{Q}$. For the Penrose tiling, one has to perform the calculation in the field

$$\mathbb{Q}(\tau, \sqrt{2+\tau}) = \left\{ a + b\sqrt{2+\tau} + c\tau + \mathrm{d}\tau\sqrt{2+\tau} \,\middle|\, a, b, c, d \in \mathbb{Q} \right\} \tag{3.7}$$

where $\tau = (1+\sqrt{5})/2$ is the golden ratio, satisfying the quadratic equation $\tau^2 = \tau + 1$. For the Ammann–Beenker case, the corresponding number field is

$$\mathbb{Q}(\lambda) = \{a + b\lambda | a, b \in \mathbb{Q}\} \tag{3.8}$$

where $\lambda = 1 + \sqrt{2}$ is the 'silver mean' that is a solution of the quadratic equation $\lambda^2 = 2\lambda + 1$. Therefore, in order to compute the occurrence frequency of a given motive c in the tiling $\mathcal{G}$, we have to determine the area of the acceptance domain carrying out the calculation in the appropriate number field. The averaged lattice constant $\langle c\,;\mathcal{G}\rangle$ is the occurrence frequency of c summed over all possible orientations of the motive. In these quasiperiodic tilings, the frequencies of motives are independent of their orientation, hence we do not need to calculate them separately, but just have to count how many orientations of the motive occur in the tiling.

Let us focus on the Penrose tiling as an example. Rotating the motive c by an angle $\pi k/5$ ($k \in \mathbb{Z}$) essentially corresponds to a rotation of the acceptance domain by $2\pi k/5$. Furthermore, the mirror image $\bar{c}$ of the motive c also occurs with the same frequency, since the corresponding acceptance domains $A_m(\bar{c})$ are just $-A_{5-m}(c)$. Therefore, in our expansion (2.5), it is advantageous to jointly consider graphs which are mirror images of each other because they give the same contribution. For this reason, we assign two symmetry factors $R \in \{1, 2, 5, 10\}$ and $S \in \{1, 2\}$ to each of these graphs, R counting the number of rotations by angles $\pi k/5$ which do not map the graph onto itself, and $S = 2$ if reflection does not map the graph onto itself or onto a rotated copy of itself, compare figures 2 and 3. The averaged lattice constant $\langle c; \mathcal{G}\rangle$, as defined above, is thus R times the area fraction obtained for a fixed orientation of the graph c. Multiplying $\langle c; \mathcal{G}\rangle$ by the factor S, we can restrict the sum in equation (2.5) to graphs that are non-equivalent under reflection.

Eventually, we have to consider all star subgraphs of the quasiperiodic tiling, corresponding to all possible fillings of loops. In contrast to the case of simple planar (periodic) lattices, a loop in the quasiperiodic tilings can have several fillings, which may occur with

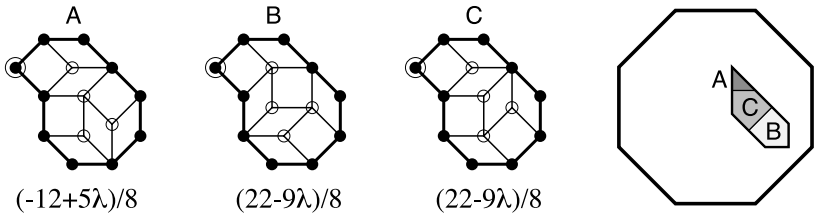

Figure 4. A loop of length ten in the Ammann–Beenker tiling that can be filled in three different ways. The corresponding occurrence frequencies of the filled patches, obtained from the area fraction of the acceptance domains shown on the right, are given below the patches. They add up to $4 - 13\lambda/8 \simeq 0.0769$ which is the frequency of the (empty) loop in the Ammann–Beenker tiling. The encircled node denotes the reference point.

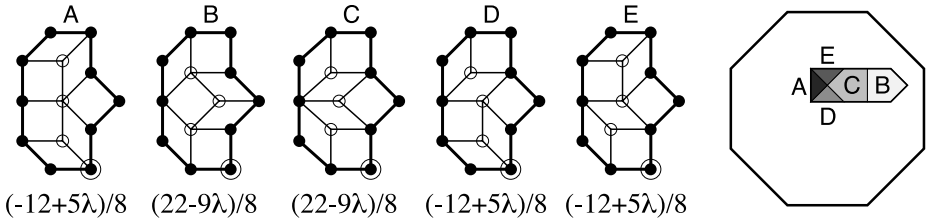

Figure 5. As figure 4, for another, reflection-symmetric loop of length ten which can be filled in five ways obtaining three reflection-symmetric patches and one pair of patches that map onto each other under reflection. Here, the frequency of the (empty) loop is $1 - 3\lambda/8 \simeq 0.0947$.

different frequencies. In figures 4 and 5, the possible fillings, together with the corresponding frequencies, of two exemplary loops in the Ammann–Beenker tiling are shown. In orthogonal space, the different fillings correspond to a dissection of the acceptance domain of the loop into non-overlapping parts, see figures 4 and 5.

In order to avoid confusion, we would like to point out once more how our frequencies are normalized, i.e., what the numbers given in figures 4 and 5 really mean. We emphasize that the frequency we compute is *not* the frequency of a particular loop of length n among all loops of the same length. Instead, it gives the probability that a randomly chosen vertex belongs to the particular loop, in an arbitrary orientation.

4. Expansion coefficients for the Penrose and the Ammann–Beenker tiling

The Penrose and the Ammann–Beenker tiling are both bipartite graphs, which means that all closed loops have an even number of edges, and at least four. Therefore, for zero magnetic field, only even powers of w occur in the expansion (2.5) that takes the form

$$F(w) = \lim_{N\to\infty} \frac{1}{N} \ln \tilde{Z}(\mathcal{G}_N) = \sum_{n=2}^{\infty} g_{2n} w^{2n} \tag{4.1}$$

where $\mathcal{G}_N$ denotes a finite patch of the quasiperiodic graph $\mathcal{G}$ containing N vertices, and $F(w)$ is, apart from a factor $-1/\beta$, the free energy per vertex. We calculated the expansion coefficients g_{2n} up to 18th order in w for both the Penrose and the Ammann–Beenker tiling. The results are presented in table 1.

As a by-product, we obtain information on another interesting model, namely the problem of self-avoiding polygons, or closed self-avoiding walks, on the quasiperiodic tiling. Self-avoiding walks and polygons have been studied extensively as simple lattice models of

Table 1. The expansion coefficients g_{2n} of the free energy of the zero-field Ising model on the Penrose and the Ammann–Beenker tiling. The values for the square lattice are included for comparison.

$2n$	Penrose tiling	Ammann–Beenker tiling	Square lattice
4	$1 = 1.00$	$1 = 1.00$	1
6	$9 - 4\tau \simeq 2.53$	$\lambda \simeq 2.41$	2
8	$12\frac{1}{2} - 4\tau \simeq 6.03$	$47\frac{1}{2} - 17\lambda \simeq 6.46$	$4\frac{1}{2}$
10	$251\frac{3}{5} - 144\frac{1}{5}\tau \simeq 18.28$	$138 - 50\lambda \simeq 17.29$	12
12	$731\frac{5}{6} - 416\tau \simeq 58.73$	$803\frac{1}{3} - 310\frac{1}{2}\lambda \simeq 53.72$	$37\frac{1}{3}$
14	$1784 - 969\tau \simeq 216.13$	$-1220 + 586\lambda \simeq 194.73$	130
16	$-27\,821\frac{3}{4} + 17\,750\tau \simeq 898.35$	$96\frac{3}{4} + 295\frac{1}{2}\lambda \simeq 810.15$	$490\frac{1}{4}$
18	$-124\,027 + 79\,078\frac{2}{3}\tau \simeq 3924.97$	$-108\,706 + 46\,566\frac{1}{3}\lambda \simeq 3715.07$	$1958\frac{2}{3}$

Table 2. The mean number (per vertex) of self-avoiding $2n$-step polygons S_{2n} on the Penrose and the Ammann–Beenker tiling, and on the square lattice.

$2n$	Penrose tiling	Ammann–Beenker tiling	Square lattice
4	$1 = 1.00$	$1 = 1.00$	1
6	$9 - 4\tau \simeq 2.53$	$\lambda \simeq 2.41$	2
8	$15 - 4\tau \simeq 8.53$	$50 - 17\lambda \simeq 8.96$	7
10	$309\frac{3}{5} - 168\frac{1}{5}\tau \simeq 37.45$	$142 - 44\lambda \simeq 35.77$	28
12	$1066 - 552\tau \simeq 172.85$	$1173 - 416\lambda \simeq 168.69$	124
14	$6400 - 3405\tau \simeq 890.59$	$1704 - 353\lambda \simeq 851.78$	588
16	$5093 - 170\tau \simeq 4817.93$	$27\,175 - 9356\lambda \simeq 4587.62$	2 938
18	$75\,115 - 29\,655\tau \simeq 27\,132.20$	$5992 + 8178\lambda \simeq 25\,735.44$	15 268

polymers or planar vesicles, see for instance [47–49]. Most investigations in the literature restrict to periodic lattices [47], only few results are known for hierarchical [48] and quasiperiodic [50] graphs. It is probably hard to justify why a quasiperiodic discretization should be of physical interest; however, one would expect that the physical properties will be very similar as those for periodic planar lattices, and that critical point properties are universal. From a mathematical point of view, the problem is interesting in the sense that one now has to average over all possible local configurations, and consequently the coefficients of the corresponding generating functions take values in certain quadratic number fields.

The quantities of interest are the sums S_{2n} of the occurrence frequencies of all order-$2n$ loops which are presented in table 2. Here, S_{2n} is nothing but the mean number per vertex of closed self-avoiding walks with $2n$ steps, i.e., random walks with $2n$ steps that never return to a vertex visited before, except for the end point which equals their starting point. For regular and recently also for 'semi-regular' lattices, there exist data for rather large values of n in the literature [49]; the square lattice numbers are series M1780 in [51]. A related problem, the enumeration of self-avoiding walks on quasiperiodic tilings, was already investigated by Briggs [50]. However, his results are based on counting walks emanating from a fixed starting point, whereas we compute the exact average over all possible starting points for the self-avoiding polygons. Note that the number of walks does depend on the initial vertex; however, the asymptotic behaviour should be independent of this choice.

The coefficients g_{2n} and S_{2n} listed in tables 1 and 2 belong to degree-two extensions of the field of rational numbers, namely $\mathbb{Q}(\tau)$ for the Penrose and $\mathbb{Q}(\lambda)$ for the Ammann–Beenker

Table 3. The number of symmetry-inequivalent closed loops of order $2n$ contributing to the high-temperature expansion and the number of patches obtained by filling the loops.

	Penrose		Ammann–Beenker		Square lattice
$2n$	empty	filled	empty	filled	empty/filled
4	2	2	2	2	1
6	6	6	4	4	1
8	24	28	17	20	3
10	143	174	77	112	6
12	839	1 034	479	743	25
14	5 634	6 957	3 007	4 981	86
16	37 677	46 712	20 175	35 063	414
18	255 658	317 028	139 146	244 638	1975

tiling, respectively. We note that for the Penrose case the frequencies of subgraphs, and thus the coefficients g_{2n} and S_{2n}, belong to the field $\mathbb{Q}(\tau)$, whereas the areas of their acceptance domains in general are elements of $\mathbb{Q}(\tau, \sqrt{2+\tau})$.

The limitation of our calculations was caused by a strong, exponential growth of the number of graphs which have to be taken into account. For the Penrose tiling, we have—even after identifying graphs that are equivalent by rotation or reflection—to deal with more than 300 000 different graphs contributing to the 18th order, see table 3, and their quantity grows approximately by a factor between six and seven when increasing the order by two. The corresponding numbers of graphs for the square lattice, included in table 3, are much smaller; the sequence of these numbers is apparently not contained in [51]. We generated the order-$2n$ loops as boundaries of patches that are constructed iteratively by successively attaching rhombi to their surface, terminating the process when attaching further rhombi does not lead to new order-$2n$ loops. By this procedure, we make sure that all graphs are found. However, we have to pay the price that topologically identical graphs are obtained repeatedly and have to be rejected, thus slowing down the procedure substantially.

5. Critical behaviour

In many cases, high-temperature expansions yield good estimates of the critical temperature and the critical exponent of the free energy. The simplest approach, which is commonly used for this purpose, uses the ratio of two successive coefficients g_{2n}/g_{2n-2} in the expansion [27]. Assuming that the free energy $F(w)$ behaves in the vicinity of the critical point w_c as

$$F(w) \sim (1 - w^2/w_c^2)^{\kappa} \tag{5.1}$$

one can easily see from (4.1) that

$$\frac{g_{2n}}{g_{2n-2}} = \frac{1}{w_c^2}\left(1 - \frac{\kappa+1}{n}\right) + \mathrm{O}(n^{-2}). \tag{5.2}$$

In other words, for sufficiently large values of n, the ratios g_{2n}/g_{2n-2} should lie on a straight line when plotted as a function of n^{-1}. The slope of this line and its displacement from the origin determine the critical point w_c and the exponent κ. Here, κ is related to the usual correlation exponent ν by $\kappa = \nu d$, where $d = 2$ is the spatial dimension.

We may estimate the critical temperature from the sequence

$$\varrho(2n) = \left[n\frac{g_{2n}}{g_{2n-2}} - (n-1)\frac{g_{2n-2}}{g_{2n-4}}\right]^{-1} \tag{5.3}$$

Table 4. Estimates of the critical point of the Ising model on the Penrose tiling and the Ammann–Beenker tiling, and on the square lattice.

	$\varrho(2n)$		
$2n$	Penrose tiling	Ammann–Beenker tiling	Square lattice
8	0.5116	0.2892	0.3333
10	0.1778	0.3725	0.2308
12	0.2430	0.1902	0.1875
14	0.1543	0.1486	0.1752
16	0.1334	0.1264	0.1726
18	0.1648	0.1252	0.1728
w_c^2	0.1563(5)[a] 0.1552(6)[b]	0.1566(5)[c]	0.1716[d]

[a] After [31].
[b] After [33].
[c] After [34].
[d] This corresponds to the exact value $w_c = \sqrt{2} - 1$ [52, 53].

that approaches w_c^2 in the limit $n \to \infty$. In table 4, we show the results for $\varrho(2n)$ for the two quasiperiodic tilings under consideration and compare these with the estimates of the critical point from Monte Carlo simulations [31, 33, 34]. The corresponding values for the square lattice are included for comparison.

As one can see, the convergence of $\varrho(2n)$ is rather poor for the quasiperiodic tilings. In general, the rate of convergence is determined by additional singularities $w_c' \in \mathbb{C}$ of $F(w)$ lying close to w_c in the complex plane. These give a correction to g_{2n}/g_{2n-2} which behaves like $\mathrm{O}[(w_c'/w_c)^{2n}]$ [27]. The influence of these corrections must be substantial in our case rendering the method rather inapplicable for us. We will come back to this point in section 6 below when we discuss the corresponding quantities for periodic approximants, compare also figure 8 that contains a plot of the ratios g_{2n}/g_{2n-2} for the case of the Penrose tiling.

There is, however, another method which is more suitable for us to examine the critical behaviour. Let us consider a sequence of partial sums F_m of the expansion (4.1) at the critical point w_c

$$F_m = \sum_{n=2}^{m} g_{2n} w_c^{2n}. \tag{5.4}$$

If the function $F(w)$ behaves like (5.1), then the asymptotic behaviour of the coefficient $\tilde{g}_{2n} = w_c^{2n} g_{2n}$ of its expansion in the variable w^2/w_c^2 is given by $\tilde{g}_{2n} \sim n^{-\kappa-1}$ for $n \to \infty$ [54, 55]. Therefore, for large m, we have

$$\begin{aligned} F_m &= F_\infty - \sum_{n=m+1}^{\infty} g_{2n} w_c^{2n} = F_\infty - \sum_{n=m+1}^{\infty} \tilde{g}_{2n} \\ &\simeq F_\infty - \tilde{b} \sum_{n=m+1}^{\infty} n^{-(\kappa+1)} \simeq F_\infty - b m^{-\kappa} \end{aligned} \tag{5.5}$$

where b is a parameter and the last relation is obtained by approximating the sum by an integral. Therefore, for sufficiently large m, the values F_m should lie on a straight line when plotted versus $m^{-\kappa}$. In figure 6, we plot the partial sums F_m for the Penrose and the Ammann–Beenker tiling, taking $\kappa = 2\nu = 2$, and w_c equal to the Monte Carlo estimates of [33, 34], see also

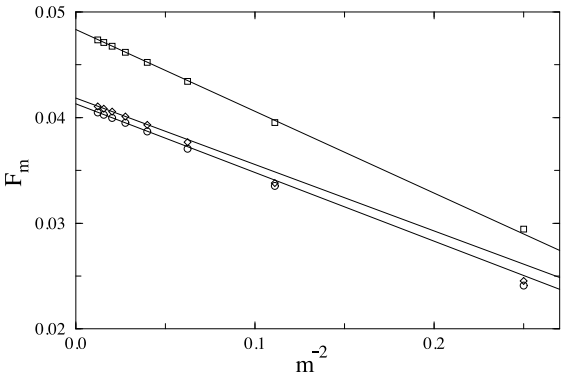

Figure 6. The dependence of the partial sums F_m of equation (5.4) on m^{-2} for the Penrose tiling (○), the Ammann–Beenker tiling (◇), and the square lattice (□), respectively. The straight lines are least-square fits to the data, disregarding the three points with smallest m values.

table 4. For comparison, we also included corresponding data for the square lattice where the exact solution is known. Apparently, the data points lie close to a straight line for all three cases, and the fluctuations in the data for the quasiperiodic tilings are not visibly larger than those for the square lattice. Thus, we conclude that our data are compatible with the Onsager universality class.

From equation (5.5), we may also try to derive estimates of the critical exponents $\nu = \kappa/2$ by solving

$$\frac{F_{m+2} - F_m}{F_m - F_{m-2}} = \frac{1 - \left(\frac{m}{m+2}\right)^{2\nu_m}}{\left(\frac{m}{m-2}\right)^{2\nu_m} - 1} \tag{5.6}$$

for the value of ν_m. Clearly, these are biased estimates since the critical temperatures have been used as an input in (5.4). In table 5, we show the values of ν_m obtained in this way. Not too surprisingly, we also recover rather strong fluctuations in these data, and no clear convergence is visible, at least for the quasiperiodic cases. Therefore, we estimate the value of ν by taking the arithmetic mean of the ν_m. The error estimates are just the standard deviation which is particularly large for the Ammann–Beenker tiling, and nowhere near the accuracy that has been reached by Monte Carlo simulations [34]. However, this procedure should be taken with a grain of salt, since the ν_m should eventually approach the correct value of ν for large m, and we did not justify why taking a mean makes sense in this case. We have also tried to use Padé approximants to extract information about the critical point and critical exponent, but this did not improve the situation—apparently our series is just too short.

Concerning the numbers of self-avoiding polygons S_{2n} shown in table 2, one considers their generating function

$$G(x) = \sum_{n=2}^{\infty} S_{2n} x^{2n} \tag{5.7}$$

which has a critical point x_c that is characterized by a cusp-like singularity; i.e., in the vicinity of x_c one has

$$G(x) \sim A(x) + B(x)(1 - x^2/x_c^2)^{2-\alpha} \tag{5.8}$$

with a critical exponent α, and $A(x)$ and $B(x)$ are non-singular at $x = x_c$. We note that the only exact result for the related problem of self-avoiding walks in two dimensions is obtained

Table 5. Estimates ν_m (5.6) of the critical exponent ν of the Ising model on the Penrose tiling and the Ammann–Beenker tiling, and on the square lattice.

	ν_m		
m	Penrose tiling	Ammann–Beenker tiling	Square lattice
6	0.922	0.749	0.864
8	0.968	1.189	1.022
10	1.208	1.267	1.043
12	1.160	1.178	1.027
14	1.021	0.987	1.011
16	1.044	0.816	1.001
ν	1.05 ± 0.11	1.03 ± 0.21	0.99 ± 0.07

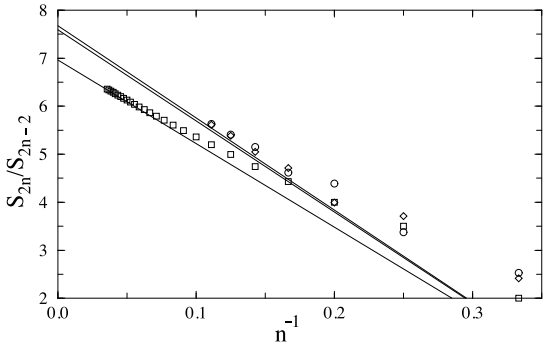

Figure 7. Ratios of the numbers of self-avoiding polygons (per vertex) on the Penrose tiling (○), the Ammann–Beenker tiling (◇), and the square lattice (□), respectively. Square lattice data for $2n \leqslant 56$ are taken from [56]. The straight lines are obtained from equation (5.8), in analogy to equation (5.2), using the critical exponent $\alpha = \frac{1}{2}$ and the approximate values of the critical point x_c given in [50] and [49].

by the Coulomb gas approach [57] and gives a critical point $x_c^2 = 1/(2 + \sqrt{2})$ and critical exponents $\alpha = \frac{1}{2}$, $\gamma = \frac{43}{32} = 1.343\,75$ and $\nu = \frac{3}{4}$ for the hexagonal lattice. Frequently, the so-called connective constant $\mu = 1/x_c$ is given instead of x_c. In [50], estimates of the critical point x_c for self-avoiding walks, which coincides with the value for self-avoiding polygons, are given based on enumerations of walks of at most 20 and 16 steps for the Penrose and the Ammann–Beenker tiling, respectively. The corresponding critical exponent in this case is γ, and all results support the conjecture that the self-avoiding walk problems on two-dimensional lattices and quasiperiodic tilings belong to the same universality class.

In figure 7, we show the ratios of successive numbers S_{2n}/S_{2n-2} as a function of $1/n$, which, by the same arguments that led to equation (5.2), should lie on a straight line for large n. Clearly, this is true for the square lattice, whereas the data for the Penrose and the Ammann–Beenker tiling still show sizable fluctuations. The straight lines in figure 7 are the functions $[1 - 5/(2n)]/x_c^2$, compare (5.2), where we used the critical exponent $\alpha = \frac{1}{2}$ and the value $\mu = 2.618\,158\,53$ cited in [49] for the square lattice connective constant, and the estimates $x_c = 0.363$ and $x_c = 0.361$ [50] for the critical points on the Penrose and the Ammann–Beenker tiling, respectively. Given the rather short sequence at our disposal, and the uncertainty in the estimates [50], the agreement for the quasiperiodic cases is reasonable, thus

supporting the conjecture that the critical point of self-avoiding polygons on such quasiperiodic tilings is described by the same critical exponents as for the hexagonal lattice [57].

6. Partition functions of periodic approximants

One may pose the question whether one can calculate the expansion coefficients g_{2n} in equation (4.1) by a different method, thus verifying our results. Perhaps it might even be possible to calculate the partition function $Z(\mathcal{G})$ on certain quasiperiodic tilings $\mathcal{G}$ exactly. Although this may seem hopeless, there exist methods to tackle this problem, which at least allow us to compute the partition function of general periodic lattices explicitly, thus also for periodic approximants of the quasiperiodic tilings. Let us briefly recall some exact results on partition functions on two-dimensional lattices.

The first solution of the two-dimensional zero-field Ising model for the square lattice had been found by Onsager and Kaufman [53, 58] in 1944. Several years later, Kac and Ward [59] developed a combinatorial approach in which the problem was reduced to the calculation of a determinant of a certain matrix K (see below) which depends on the lattice and the coupling constants between the spins. Although this approach was not rigorous, it appeared extremely plausible and it initiated numerous attempts to generalize this result to other lattices [60–63]. Recently, Dolbilin *et al* [64] proved the long-known formula

$$\tilde{Z}(\mathcal{G})^2 = \det(K) \tag{6.1}$$

for a zero-field Ising model on an arbitrary planar graph $\mathcal{G}$ with arbitrary (in general site-dependent) spin coupling constants. The matrix elements $K(\boldsymbol{e}_i, \boldsymbol{e}_j)$ of the $2M \times 2M$ matrix K are labelled by oriented edges $\boldsymbol{e}_i$ and $\boldsymbol{e}_j$, $1 \leqslant i, j \leqslant 2M$. They are defined as

$$K(\boldsymbol{e}_i, \boldsymbol{e}_j) = \begin{cases} 1 & \text{if} \quad \boldsymbol{e}_i = \boldsymbol{e}_j \\ -w_i \exp\left[\dfrac{\mathrm{i}}{2}(\widehat{\boldsymbol{e}_i, \boldsymbol{e}_j})\right] & \text{if} \quad f(\boldsymbol{e}_i) = b(\boldsymbol{e}_j) \quad \text{and} \quad f(\boldsymbol{e}_j) \neq b(\boldsymbol{e}_i) \\ 0 & \text{otherwise} \end{cases} \tag{6.2}$$

where $w_i = \tanh(\beta J_i)$ and J_i is the spin coupling constant along the edge $\boldsymbol{e}_i$, which is independent of the edge in our case, $J_i \equiv J$. Furthermore, $(\widehat{\boldsymbol{e}_i, \boldsymbol{e}_j})$ denotes the angle between edges $\boldsymbol{e}_i$ and $\boldsymbol{e}_j$, and $b(\boldsymbol{e}_i)$ and $f(\boldsymbol{e}_i)$ are the starting point and the end point of the edge $\boldsymbol{e}_i$, respectively. If $\mathcal{G}$ is periodic, the matrix K is cyclic and the determinant can be calculated exactly in the thermodynamic limit $M \to \infty$. We can therefore apply (6.2) and calculate $\tilde{Z}(\mathcal{G})$ exactly for periodic approximants of the Penrose and the Ammann–Beenker tiling.

Let us now briefly describe how to generate periodic approximants of quasiperiodic tilings in the framework of the cut-and-project method discussed in section 3. The acceptance domain A and the projection onto perpendicular space $E_\perp$ are altered in a way that corresponds to replacing the irrational numbers τ and λ by rational approximants τ_m and λ_m. Here, for the Penrose tiling we use $\tau_m = f_{m+1}/f_m$ where $f_{m+1} = f_m + f_{m-1}$, and $f_0 = 0$, $f_1 = 1$ are the Fibonacci numbers, and $\lim_{m\to\infty} \tau_m = \tau$. Analogously, one defines rational approximants $\lambda_m = g_{m+1}/g_m$ with the 'octonacci numbers' $g_{m+1} = 2g_m + g_{m-1}$ and $g_0 = 0$, $g_1 = 1$, and $\lim_{m\to\infty} \lambda_m = \lambda$ for the case of the Ammann–Beenker tiling.

In this way, one obtains periodic approximants of the Penrose tiling with unit cells containing $\mathcal{N} = 11, 29, 76, 199, 521, 1364, 3571, 9349$ vertices for $m = 1, 2, 3, 4, 5, 6, 7, 8$, respectively. The unit cells of the periodic approximants of the Ammann–Beenker tiling with $m = 1, 2, 3, 4, 5$ contain $\mathcal{N} = 7, 41, 239, 1393, 8119$ vertices. For both tilings, the number of oriented edges is $2M = 4\mathcal{N}$, because each vertex has exactly four neighbours. We note that the approximant $m + 1$ contains about $\tau^2 = \tau + 1 \simeq 2.618$ and $\lambda^2 = 2\lambda + 1 \simeq 5.828$

as many vertices and bonds as the approximant m for the Penrose and the Ammann–Beenker case, respectively.

For each periodic approximant, we define a matrix $\tilde{K}$ labelled by oriented edges e'_i and e'_j with starting point in the unit cell. It is related to the Kac–Ward matrix K (6.2) as

$$\tilde{K}(e'_i, e'_j) := K(e_i, e_j) \exp(-\mathrm{i}k_1\Delta_1) \exp(-\mathrm{i}k_2\Delta_2). \tag{6.3}$$

Here, we can assume that $e'_i = e_i$ starts in the unit cell, and e'_j equals e_j modulo the unit cell, i.e., if $b(e_j) = \xi_j V + \eta_j W$, where V and W are the base vectors spanning the unit cell, then $b(e'_j) = \mathrm{frac}(\xi_j)V + \mathrm{frac}(\eta_j)W$ where $\mathrm{frac}(x)$ denotes the fractional part of x. The integers Δ_1 and Δ_2 are the integer parts $\lfloor \xi_j \rfloor$ and $\lfloor \eta_j \rfloor$, respectively, and $\tilde{K}$ depends on the 'wavevectors' k_1 and k_2 which are real numbers. Due to the fact that the Kac–Ward matrix K of the periodic approximant is cyclic, its determinant can be expressed as a product of the determinant of $\tilde{K}$ over all values of k_1 and k_2, corresponding to a reduction to the unit cell. Calculating the logarithm of $\tilde{Z}(\mathcal{G})$, and taking relation (6.1) into account, one obtains

$$\ln \tilde{Z}(\mathcal{G}) = \frac{1}{8\pi^2} \int_0^{2\pi} \int_0^{2\pi} \ln \det \tilde{K}(k_1, k_2)\, \mathrm{d}k_1\, \mathrm{d}k_2. \tag{6.4}$$

Let us now expand this equation in a series with respect to w and compare it with the high-temperature expansion (4.1). For this purpose, we exploit the fact (6.2) that the (finite-dimensional) matrix $\tilde{K}(k_1, k_2)$ has a form $\tilde{K}(k_1, k_2) = 1 + w\tilde{L}(k_1, k_2)$ where $\tilde{L}(k_1, k_2)$ has zero trace. Therefore, using

$$\begin{aligned} \det[1 + w\tilde{L}(k_1, k_2)] &= \det \exp \ln[1 + w\tilde{L}(k_1, k_2)] \\ &= \exp \mathrm{tr} \ln[1 + w\tilde{L}(k_1, k_2)] \end{aligned} \tag{6.5}$$

one obtains, expanding the logarithm in powers of $w\tilde{L}(k_1, k_2)$,

$$\begin{aligned} \ln \det \tilde{K}(k_1, k_2) &= \mathrm{tr} \ln[1 + w\tilde{L}(k_1, k_2)] \\ &= \sum_{p=1}^{\infty} \frac{(-1)^{p+1}}{p} \mathrm{tr}[\tilde{L}^p(k_1, k_2)] w^p \end{aligned} \tag{6.6}$$

where, again, only even values of p yield non-vanishing contributions to the sum. Comparing this result with equation (6.4), we derive an expression for the coefficient g_{2n} in the expansion (4.1)

$$g_{2n} = -\frac{1}{16\pi^2 n} \int_0^{2\pi} \int_0^{2\pi} \mathrm{tr}[\tilde{L}^{2n}(k_1, k_2)]\, \mathrm{d}k_1\, \mathrm{d}k_2 \tag{6.7}$$

for the periodic approximants. We have calculated the coefficients from (6.7) for the leading orders in w for both the Penrose and the Ammann–Beenker tiling. The limitation of the calculation was due to a rapidly growing dimension of the complex matrix $\tilde{L}(k_1, k_2)$, which was equal to 37 396 and 32 476 for our largest approximants of the Penrose and Ammann–Beenker tiling, respectively. The results are presented in tables 6 and 7. Clearly, with increasing size of the approximant, the coefficients approach those of the quasiperiodic system, and the coefficients of the largest approximant are already quite close to those of the quasiperiodic case.

We now consider the ratios (5.2) for the periodic approximants of the Penrose tiling. The result is shown in figure 8. Although we included terms up to order $2n = 56$, the data for the two periodic approximants do not lie on straight lines, in contrast to those of the square lattice. Instead, they show large fluctuations, and apparently the fluctuations for the smallest approximant with 11 vertices in the unit cell turn out to be much larger than those for the larger approximant which contains 29 vertices. It would be interesting to have a better understanding

Table 6. Expansion coefficients of the free energy for the Ising model on the Penrose tiling and its periodic approximants $m = 1, 2, \ldots, 8$ with $\mathcal{N}$ vertices in a unit cell.

m	$\mathcal{N}$	$2M$	g_4	g_6	g_8
1	11	44	1	$25/11 \simeq 2.2727$	$127/22 \simeq 5.7727$
2	29	116	1	$73/29 \simeq 2.5172$	$349/58 \simeq 6.0172$
3	76	304	1	$5/2 \simeq 2.5000$	$227/38 \simeq 5.9737$
4	199	796	1	$503/199 \simeq 2.5276$	$2399/398 \simeq 6.0276$
5	521	2 084	1	$1315/521 \simeq 2.5240$	$6273/1042 \simeq 6.0202$
6	1364	5 456	1	$862/341 \simeq 2.5279$	$4111/682 \simeq 6.0279$
7	3571	14 284	1	$9025/3571 \simeq 2.5273$	$43\,043/7142 \simeq 6.0267$
8	9349	37 396	1	$23\,633/9349 \simeq 2.5279$	$112\,709/18\,698 \simeq 6.0279$
∞	∞	∞	1	$9 - 4\tau \simeq 2.5279$	$12\frac{1}{2} - 4\tau \simeq 6.0279$

m	g_{10}	g_{12}	g_{14}
1	$175/11 \simeq 15.909$	$3145/66 \simeq 47.652$	$1812/11 \simeq 164.73$
2	$504/29 \simeq 17.379$	$341/6 \simeq 56.833$	$6011/29 \simeq 207.27$
3	$679/38 \simeq 17.868$	$6629/114 \simeq 58.149$	$16\,123/76 \simeq 212.14$
4	$3624/199 \simeq 18.211$	$69\,833/1194 \simeq 58.487$	$42\,552/199 \simeq 213.83$
5	$9496/521 \simeq 18.226$	$610\,783/10\,420 \simeq 58.616$	$112\,451/521 \simeq 215.84$
6	$24\,921/1364 \simeq 18.271$	$160\,129/2728 \simeq 58.698$	$294\,347/1364 \simeq 215.80$
7	$65\,249/3571 \simeq 18.272$	$1\,258\,025/21\,426 \simeq 58.715$	$771\,636/3571 \simeq 216.08$
8	$170\,887/9349 \simeq 18.279$	$3\,293\,987/56\,094 \simeq 58.723$	$2\,020\,105/9349 \simeq 216.08$
∞	$251\frac{3}{5} - 144\frac{1}{5}\tau \simeq 18.279$	$731\frac{5}{6} - 416\tau \simeq 58.731$	$1784 - 969\tau \simeq 216.13$

m	g_{16}	g_{18}
1	$29\,439/44 \simeq 669.07$	$95\,119/33 \simeq 2882.4$
2	$100\,769/116 \simeq 868.70$	$342\,484/87 \simeq 3936.6$
3	$33\,325/38 \simeq 876.97$	$222\,817/57 \simeq 3909.1$
4	$709\,087/796 \simeq 890.81$	$2\,345\,981/597 \simeq 3929.6$
5	$1\,867\,989/2084 \simeq 896.35$	$6\,128\,605/1563 \simeq 3921.1$
6	$1\,223\,683/1364 \simeq 897.13$	$4\,015\,369/1023 \simeq 3925.1$
7	$12\,827\,639/14\,284 \simeq 898.04$	$42\,041\,215/10\,713 \simeq 3924.3$
8	$33\,589\,237/37\,396 \simeq 898.20$	$110\,077\,367/28\,047 \simeq 3924.7$
∞	$-27\,821\frac{3}{4} + 17\,750\tau \simeq 898.35$	$-124\,027 + 79\,078\frac{2}{3}\tau \simeq 3925.0$

Table 7. As table 6, but for approximants $m = 1, 2, 3, 4, 5$ of the Ammann–Beenker tiling.

m	$\mathcal{N}$	$2M$	g_4	g_6	g_8
1	7	28	1	$17/7 \simeq 2.428\,57$	$87/14 \simeq 6.214\,29$
2	41	164	1	$99/41 \simeq 2.414\,63$	$529/82 \simeq 6.451\,22$
3	239	956	1	$577/239 \simeq 2.414\,23$	$3087/478 \simeq 6.458\,16$
4	1393	5572	1	$3363/1393 \simeq 2.414\,21$	$17\,993/2786 \simeq 6.458\,36$
5	8119	32 476	1	$19\,601/8119 \simeq 2.414\,21$	$104\,871/16\,238 \simeq 6.458\,37$
∞	∞	∞	1	$\lambda \simeq 2.414\,21$	$47\frac{1}{2} - 17\lambda \simeq 6.458\,37$

m	g_{10}	g_{12}	g_{14}
1	$115/7 \simeq 16.4286$	$2189/42 \simeq 52.1190$	$1395/7 \simeq 199.286$
2	$708/41 \simeq 17.2683$	$13\,183/246 \simeq 53.5894$	$7994/41 \simeq 194.976$
3	$4132/239 \simeq 17.2887$	$77\,029/1434 \simeq 53.7162$	$46\,542/239 \simeq 194.736$
4	$24\,084/1393 \simeq 17.2893$	$74\,832/1393 \simeq 53.7200$	$271\,258/1393 \simeq 194.729$
5	$140\,372/8119 \simeq 17.2893$	$113\,779/2118 \simeq 53.7200$	$1\,581\,006/8119 \simeq 194.729$
∞	$138 - 50\lambda \simeq 17.2893$	$803\frac{1}{3} - 310\frac{1}{2}\lambda \simeq 53.7200$	$-1220 + 586\lambda \simeq 194.729$

m	g_{16}	g_{18}
1	$22\,815/28 \simeq 814.821$	$78\,479/21 \simeq 3737.10$
2	$132\,885/164 \simeq 810.274$	$153\,121/41 \simeq 3734.66$
3	$774\,507/956 \simeq 810.154$	$2\,664\,121/717 \simeq 3715.65$
4	$4\,514\,157/5572 \simeq 810.150$	$739\,303/199 \simeq 3715.09$
5	$26\,310\,435/32\,476 \simeq 810.150$	$90\,488\,057/24\,357 \simeq 3715.07$
∞	$96\frac{3}{4} + 295\frac{1}{2}\lambda \simeq 810.150$	$-108\,706 + 46\,566\frac{1}{3}\lambda \simeq 3715.07$

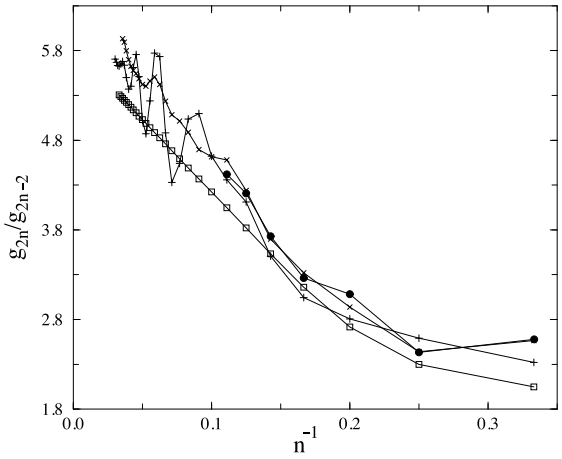

Figure 8. The ratios g_{2n}/g_{2n-2} of expansion coefficients for the square lattice (□), the first (+) and the second (×) periodic approximant of the Penrose tiling, and for the Penrose tiling (●), respectively. Lines are meant as guides to the eye only.

of this phenomenon, perhaps an investigation of the complex-temperature phase diagram of the periodic approximants can give an explanation of this observation. Again, figure 8 also shows that the data for the second approximant are already rather close to that of the quasiperiodic tiling, and one might conclude from figure 8 that the fluctuations in the ratios of expansion coefficients become less with increasing size of the approximant.

7. Conclusions

We considered the Ising model on two planar quasiperiodic graphs, the Penrose and the Ammann–Beenker tiling. We calculated the leading terms of the high-temperature expansion of the free energy exactly, using the embedding of the quasiperiodic tilings into higher-dimensional periodic lattices to compute the occurrence frequencies of patterns in the tiling. These frequencies are expressed in terms of characteristic quadratic irrationalities related to ten- and eightfold rotational symmetry, the golden mean $\tau = (1 + \sqrt{5})/2$ and the silver mean $\lambda = 1 + \sqrt{2}$ for the Penrose and the Ammann–Beenker tiling, respectively.

The number of graphs that contribute to a given order in the expansion grows much faster with the order than for a simple periodic lattice, therefore we did not go beyond the 18th order in the expansion variable $w = \tanh(\beta J)$ in this work. From our expansion alone, it is difficult to extract information about the critical behaviour. However, using estimates of the critical temperature obtained by other methods to analyse our data, we find that our expansions are in accordance with the conjecture that Ising models on such planar quasiperiodic graphs belong to the Onsager universality class.

In order to compute the expansion coefficients, we had to construct all polygons on the quasiperiodic graphs with up to $2n = 18$ edges. Thus, we obtain the average number of such self-avoiding polygons as a by-product of our calculation. Comparison with earlier results on self-avoiding walks [50], based on enumerating walks that start from a chosen vertex in the tiling, indicates that the self-avoiding polygons on the examples we considered belong to the same universality class. In particular, this means that the corresponding critical point is described by the same exponents as for the hexagonal lattice which are known analytically [57].

Finally, we considered periodic approximants of the quasiperiodic tilings. For these, in principle, it is possible to compute the free energy of the infinite periodic system analytically. Here, we are only interested in the leading terms of the free energy, which we compare with those of the infinite quasiperiodic tiling. We find that, at least for the leading orders in w, the rational coefficients of the approximants converge rapidly towards the irrational coefficients obtained for the quasiperiodic tiling. However, we also find that the series expansions for periodic approximants, which can be performed to higher order, show strong fluctuations, as can been seen in figure 8. Although there is some indication that these fluctuations might be less dramatic for the quasiperiodic tiling, remnants of these fluctuations will certainly survive.

In conclusion, it is doubtful whether the computational effort necessary to extend the expansions to higher order will result in a considerable improvement of the estimates of the critical properties. Besides the technical difficulties arising from the huge number of graphs that have to be taken into account, and the averaging with the occurrence frequencies of the graphs in the infinite quasiperiodic tiling, it finally turns out that the hard-earned series coefficients do not reward us for our labour: their behaviour is not as regular as for the square lattice, showing strong fluctuations that make any extrapolation extremely difficult. For this reason, we neither expect that one can learn much from the analogous procedure for the magnetic susceptibility, because the computation of the corresponding high-temperature series, though possible by similar means, is even more laborious because more general graphs contribute in this case. Instead, it might be more rewarding to consider periodic approximants and use methods such as those outlined in section 6 and [65] to compute physical quantities, such as for instance the magnetization or correlation functions. At least, we can compute the exact values of the critical temperatures for periodic approximants, and thus derive very precise estimates for the critical temperature of the quasiperiodic cases, as we shall show in a forthcoming publication.

Acknowledgments

We thank M Baake for discussions and useful comments. Financial support by Deutsche Forschungsgemeinschaft (DFG) is gratefully acknowledged.

References

[1] Schechtman D, Blech I, Gratias D and Cahn J W 1984 Metallic phase with long-range orientational order and no translational symmetry *Phys. Rev. Lett.* **53** 1951–3

[2] Ishimasa T, Nissen H-U and Fukano Y 1985 New ordered state between crystalline and amorphous in Ni–Cr particles *Phys. Rev. Lett.* **55** 511–13

[3] Bendersky L 1985 Quasicrystals with one-dimensional translational symmetry and a tenfold rotation axis *Phys. Rev. Lett.* **55** 1461–3

[4] Wang N, Chen H and Kuo K H 1987 Two-dimensional quasicrystal with eightfold rotational symmetry *Phys. Rev. Lett.* **59** 1010–13

[5] Berger C 1994 Electronic properties of quasicrystals experimental *Lectures on Quasicrystals* ed F Hippert and D Gratias (Les Ulis: Les Editions de Physique) pp 463–504

[6] Athanasiou N S 1997 Formation, characterization and magnetic properties of some ternary Al–Cu–M (M equals transition metal) quasicrystals prepared by conventional solidification *Int. J. Mod. Phys.* B **11** 2443–64

[7] Yokoyama Y, Inoue A and Masumoto T 1992 New ferrimagnetic quasicrystals in Al–Pd–Mn–B and Al–Cu–Mn–B systems *Mater. Trans.* **33** 1012–19

[8] Lyubutin I S, Lin C R and Lin S T 1997 Magnetic ordering of Fe atoms in icosahedral $Al_{70-x}B_xPd_{30-y}Fe_y$ quasicrystals *J. Exp. Theor. Phys.* **84** 800–7

[9] Charrier B, Ouladdiaf B and Schmitt D 1997 Observation of quasimagnetic structures in rare-earth-based icosahedral quasicrystals *Phys. Rev. Lett.* **78** 4637–40

Charrier B, Ouladdiaf B and Schmitt D 1997 Quasi-periodic antiferromagnetic order in i-$R_8Mg_{42}Zn_{50}$ (R = Tb, Dy) quasi-crystals *Physica* B **241** 733–5

Charrier B and Schmitt D 1997 Magnetic properties of $R_8Mg_{42}Zn_{50}$ quasicrystals (R = Tb, Dy, Ho, Er) *J. Magn. Magn. Mater.* **171** 106–12

Charrier B, Schmitt D and Ouladdiaf B 1998 Quasimagnetism in i–$R_8Mg_{42}Zn_{50}$ quasicrystals (R = Tb, Dy, Ho, Er) *Proc. 6th Int. Conf. on Quasicrystals (Tokyo 1997)* ed S Takeuchi and T Fujiwara (Singapore: World Scientific) pp 611–14

[10] Gavilano J L, Ambrosini B, Vonlanthen P, Chernikov M A and Ott H R 1997 Low-temperature nuclear magnetic resonance studies of an $Al_{70}Re_{8.6}Pd_{21.4}$ icosahedral quasicrystal *Phys. Rev. Lett.* **79** 3058–61

[11] Noakes D R, Kalvius G M, Wappling R, Stronach C E, White M F, Saito H and Fukamichi K 1998 Spin dynamics and freezing in magnetic rare-earth quasicrystals *Phys. Lett.* A **238** 197–202

[12] Peng D L, Sumiyama K, Suzuki K, Inoue A, Yokoyama Y, Fukaura K and Sunada H 1998 Low-temperature magnetic properties of Al–Pd–Mn–B quasicrystalline alloys *J. Magn. Magn. Mater.* **184** 319–29

[13] Simonet V, Hippert F, Audier M and Trambly de Laissardière G 1998 Origin of magnetism in crystalline and quasicrystalline AlMn and AlPdMn phase *Phys. Rev.* B **58** 8865–8

[14] Islam Z, Fisher I R, Zarestky J, Canfield P C, Stassis C and Goldman A I 1998 Reinvestigation of long-range magnetic ordering in icosahedral Tb–Mg–Zn *Phys. Rev.* B **57** 11 047–50

[15] Sato T J, Takakura H, Tsai A P and Shibata K 1998 Anisotropic spin correlations in the Zn–Mg–Ho icosahedral quasicrystals *Phys. Rev. Lett.* **81** 2364–7

[16] Grimm U and Baake M 1997 Aperiodic Ising models *The Mathematics of Long-Range Aperiodic Order* ed R V Moody (Dordrecht: Kluwer) pp 199–237

[17] Lifshitz R 1998 Symmetry of magnetically ordered quasicrystals *Phys. Rev. Lett.* **80** 2717–20

[18] Luck J M 1993 A classification of critical phenomena on quasi-crystals and other aperiodic structures *Europhys. Lett.* **24** 359–64

[19] Harris A B 1974 Effect of random defects on the critical behaviour of Ising models *J. Phys. C: Solid State Phys.* **7** 1671–92

[20] Hermisson J 1999 Aperiodische Ordnung und magnetische Phasenübergänge *Dissertation* University of Tübingen

[21] Baake M, Grimm U, Repetowicz P and Joseph D 1998 Coordination sequences and critical points *Proc. 6th Int. Conf. on Quasicrystals (Tokyo 1997)* ed S Takeuchi and T Fujiwara (Singapore: World Scientific) pp 124–7

[22] Penrose R 1974 The rôle of aesthetics in pure and applied mathematical research *Bull. Inst. Math. Appl.* **10** 266–71

[23] de Bruijn NG 1981 Algebraic theory of Penrose's non-periodic tilings of the plane I *Indagationes Mathematicae (Proc. Kon. Ned. Akad. Wet. Ser. A)* **84** 39–52

de Bruijn NG 1981 Algebraic theory of Penrose's non-periodic tilings of the plane II *Indagationes Mathematicae (Proc. Kon. Ned. Akad. Wet. Ser. A)* **84** 53–66

[24] Ammann R, Grünbaum B and Shephard G C 1992 Aperiodic tiles *Discr. Comput. Geom.* **8** 1–25

[25] Duneau M, Mosseri R and Oguey C 1989 Approximants of quasiperiodic structures generated by the inflation mapping *J. Phys. A: Math. Gen.* **22** 4549–64

[26] Katz A 1995 Matching rules and quasiperiodicity: the octagonal tiling *Beyond Quasicrystals* ed F Axel and D Gratias (Berlin: Springer) pp 141–89

[27] Domb C 1974 Ising model *Phase Transitions and Critical Phenomena* vol 3, ed C Domb and M S Green (London: Academic) pp 357–458

[28] Abe R and Dotera T 1989 High temperature expansion for the Ising model on the Penrose lattice *J. Phys. Soc. Japan* **58** 3219–26

[29] Dotera T and Abe R 1990 High-temperature expansion for the Ising model on the dual Penrose lattice *J. Phys. Soc. Japan* **59** 2064–77

[30] Miyazima S 1991 Why the critical temperature of Ising spin system in Penrose lattice is higher than that of the square lattice *Quasicrystals (Proc. China–Japan Seminars in Tokyo 1989 and Beijing 1990)* ed K H Kuo and T Ninomiya (Singapore: World Scientific) pp 386–92

[31] Okabe Y and Niizeki K 1988 Monte Carlo simulation of the Ising model on the Penrose lattice *J. Phys. Soc. Japan* **57** 16–19

[32] Okabe Y and Niizeki K 1988 Duality in the Ising model on quasicrystals *J. Phys. Soc. Japan* **57** 1536–9

[33] Sørensen E S, Jarić M V and Ronchetti M 1991 Ising model on the Penrose lattice: boundary conditions *Phys. Rev.* B **44** 9271–82

[34] Ledue D, Landau D P and Teillet J 1995 Static critical behavior of the ferromagnetic Ising model on the quasiperiodic octagonal tiling *Phys. Rev.* B **51** 12 523–30

[35] Baake M, Grimm U and Baxter R J 1994 A critical Ising model on the labyrinth *Int. J. Mod. Phys.* B **8** 3579–600

[36] Choy T C 1988 Ising models on two-dimensional quasi-crystals: some exact results *Int. J. Mod. Phys.* B **2** 49–63

[37] Lee T D and Yang C N 1952 Statistical theory of equations of state and phase transitions. II. Lattice gas and

Ising model *Phys. Rev.* **87** 410–19
[38] Simon H and Baake M 1997 Lee–Yang zeros in the scaling region of a two-dimensional quasiperiodic Ising model *J. Phys. A: Math. Gen.* **30** 5319–27
[39] Simon H 1997 Ferromagnetische Spinsysteme auf aperiodischen Strukturen *Dissertation* University of Tübingen (Darmstadt: DDD)
[40] Bose I 1987 Renormalization group (RG) study of the Ising model on higher-dimensional ($d > 1$) quasi-lattices *Phys. Lett.* A **123** 224–6
Aoyama H and Odagaki T 1987 Eight-parameter renormalization group for Penrose lattices *J. Stat. Phys.* **48** 503–11
Aoyama H and Odagaki T 1988 Renormalization group analysis of the Ising model on two-dimensional quasi-lattices *Int. J. Mod. Phys.* B **2** 13–35
[41] Hermisson J, Grimm U and Baake M 1997 Aperiodic Ising quantum chains *J. Phys. A: Math. Gen.* **30** 7315–35
[42] Hermisson J and Grimm U 1998 Surface properties of aperiodic Ising quantum chains *Phys. Rev.* B **57** R673–6
[43] Ledue D, Boutry T, Landau D P and Teillet J 1997 Finite-size behavior of the three-state Potts model on the quasiperiodic octagonal tiling *Phys. Rev.* B **56** 10 782–5
[44] Duneau M and Katz A 1985 Quasiperiodic patterns *Phys. Rev. Lett.* **54** 2688–91
[45] Baake M, Kramer P, Schlottmann M and Zeidler D 1990 Planar patterns with fivefold symmetry as sections of periodic structures in 4-space *Int. J. Mod. Phys.* B **4** 2217–68
[46] Hof A 1998 Uniform distribution and the projection method *Quasicrystals and Discrete Geometry* ed J Patera (Providence, RI: American Mathematical Society)
[47] Enting I G 1980 Generating functions for enumerating self-avoiding rings on the square lattice *J. Phys. A: Math. Gen.* **13** 3713–22
Prentis J J 1984 Crossover between random and self-avoiding behaviour in a ring polymer *J. Appl. Phys.* **17** 1723–33
Enting I G and Guttmann A J 1985 Self-avoiding polygons on the square, L and Manhattan lattices *J. Phys. A: Math. Gen.* **18** 1007–17
Privman V and Rudnick J 1985 Size of rings in two dimensions *J. Phys. A: Math. Gen.* **18** L789–93
Manna S S 1987 Directed self-avoiding polygons *J. Phys. A: Math. Gen.* **20** 2227–31
Guttmann A J and Enting I G 1988 The size and number of rings on the square lattice *J. Phys. A: Math. Gen.* **21** L165–72
Cardy J L 1988 Universal amplitude in the sizes of rings in two dimensions *J. Phys. A: Math. Gen.* **21** L797–9
Enting I G and Guttmann A J 1989 Polygons on the honeycomb lattice *J. Phys. A: Math. Gen.* **22** 1371–84
Camacho C J and Fisher M E 1990 Tunable fractal shapes in self-avoiding polygons and planar vesicles *Phys. Rev. Lett.* **65** 9–12
Fisher M E, Guttmann A J and Whittington S G 1991 Two-dimensional lattice vesicles and polygons *J. Phys. A: Math. Gen.* **24** 3095–106
Enting I G and Guttmann A J 1992 Self-avoiding rings on the triangular lattice *J. Phys. A: Math. Gen.* **25** 2791–807
Cardy J L and Guttmann A J 1993 Universal amplitude combinations for self-avoiding walks, polygons and trails *J. Phys. A: Math. Gen.* **26** 2485–94
Bennett-Wood D, Enting I G, Gaunt D S, Guttmann A J, Leask J L, Owczarek A L and Whittington S G 1998 Exact enumeration study of free energies of interacting polygons and walks in two dimensions *J. Phys. A: Math. Gen.* **31** 4725–41
Guitter E and Orlandini E 1999 Monte Carlo results for projected self-avoiding polygons: A two-dimensional model for knotted polymers *J. Phys. A: Math. Gen.* **32** 1359–85
[48] Di Stasio M, Seno F and Stella A L 1992 Vesicles on a hierarchical lattice: an exact renormalization group approach *J. Phys. A: Math. Gen.* **25** 3891–9
[49] Jensen I and Guttmann A J 1998 Self-avoiding walks, neighbour-avoiding walks and trails on semiregular lattices *J. Phys. A: Math. Gen.* **31** 8137–45
[50] Briggs K 1993 Self-avoiding walks on quasi-lattices *Int. J. Mod. Phys.* B **7** 1569–75
[51] Sloane N J A and Plouffe S 1995 *The Encyclopedia of Integer Sequences* (San Diego, CA: Academic)
[52] Kramers H A and Wannier G H 1941 Statistics of the two-dimensional ferromagnet. Part I *Phys. Rev.* **60** 252–62
[53] Onsager L 1944 Crystal statistics. I. A two-dimensional model with an order-disorder transition *Phys. Rev.* **65** 117–49
[54] Abe R 1987 Some remarks on high-temperature expansion for a certain $n = 0$ system *Prog. Theor. Phys.* **78** 97–104
[55] Abe R, Dotera T and Ogawa T 1990 Critical compressibility factor of two-dimensional lattice gas *Prog. Theor. Phys.* **84** 425-35

[56] Guttmann A J 1989 Asymptotic analysis of power-series expansions *Phase Transitions and Critical Phenomena* vol 13, ed C Domb and J L Lebowitz (London: Academic) pp 1–234

[57] Nienhuis B 1982 Exact critical point and critical exponents of $O(n)$ models in two dimensions *Phys. Rev. Lett.* **49** 1062–5

Nienhuis B 1984 Critical behavior of two-dimensional spin models and charge asymmetry in the Coulomb gas *J. Stat. Phys.* **34** 731–61

Nienhuis B 1987 Coulomb gas representations of phase transitions in two dimensions *Phase Transitions and Critical Phenomena* vol 11, ed C Domb and J L Lebowitz (London: Academic) pp 1–53

[58] Kaufman B 1949 Crystal statistics. II. Partition function evaluated by spinor analysis *Phys. Rev.* **76** 1232–43

[59] Kac M and Ward J C 1952 Combinatorial solution of the 2-dimensional Ising model *Phys. Rev.* **88** 1332–7

[60] Potts R B and Ward J C 1955 The combinatorial method and the two-dimensional Ising model *Prog. Theoret. Phys. (Kyoto)* **13** 38–46

[61] Sherman S 1960 Combinatorial aspects of the Ising model of ferromagnetism. I. A conjecture of Feynman on paths and graphs *J. Math. Phys.* **1** 202–17

[62] Burgoyne P N 1963 Remarks on the combinatorial approach to the Ising problem *J. Math. Phys.* **4** 1320–6

[63] Vdovichenko N V 1964 A calculation of the partition function for a plane dipole lattice *J. Exp. Teor. Phys.* **47** 715–9 (Engl. transl. 1965 *Sov. Phys.–JETP* **20** 477–9)

[64] Dolbilin N P, Zinowiev J M, Mishchenko A C, Shtanko M A and Shtogrin M I 1998 The Kac–Ward determinant *Proc. Steklov Institute of Mathematics* to appear

Dolbilin N P, Zinowiev J M, Mishchenko A C, Shtanko M A and Shtogrin M I 1998 Combinatorial method of Kac–Ward *Russ. Math. Surv.* to appear

[65] Vdovichenko N V 1965 Spontaneous magnetization of a plane dipole lattice *J. Exp. Theor. Phys.* **48** 527–30 (Engl. transl. 1965 *Sov. Phys.–JETP* **21** 350–2)